

## NRC Publications Archive Archives des publications du CNRC

### Response surface models for the hydrodynamic loads measured on slender underwater vehicles during pure yaw manoeuvres

Azarsina, F.; Williams, C. D.; Bachmayer, R.

This publication could be one of several versions: author's original, accepted manuscript or the publisher's version. /  
La version de cette publication peut être l'une des suivantes : la version prépublication de l'auteur, la version acceptée du manuscrit ou la version de l'éditeur.

#### Publisher's version / Version de l'éditeur:

*15th International Symposium on Unmanned Untethered Submersible Technology [Proceedings], 2007*

#### NRC Publications Archive Record / Notice des Archives des publications du CNRC :

<https://nrc-publications.canada.ca/eng/view/object/?id=d57ae627-d2eb-4f40-80c7-8073df82172a>

<https://publications-cnrc.canada.ca/fra/voir/objet/?id=d57ae627-d2eb-4f40-80c7-8073df82172a>

Access and use of this website and the material on it are subject to the Terms and Conditions set forth at

<https://nrc-publications.canada.ca/eng/copyright>

READ THESE TERMS AND CONDITIONS CAREFULLY BEFORE USING THIS WEBSITE.

L'accès à ce site Web et l'utilisation de son contenu sont assujettis aux conditions présentées dans le site

<https://publications-cnrc.canada.ca/fra/droits>

LISEZ CES CONDITIONS ATTENTIVEMENT AVANT D'UTILISER CE SITE WEB.

**Questions?** Contact the NRC Publications Archive team at

PublicationsArchive-ArchivesPublications@nrc-cnrc.gc.ca. If you wish to email the authors directly, please see the first page of the publication for their contact information.

**Vous avez des questions?** Nous pouvons vous aider. Pour communiquer directement avec un auteur, consultez la première page de la revue dans laquelle son article a été publié afin de trouver ses coordonnées. Si vous n'arrivez pas à les repérer, communiquez avec nous à PublicationsArchive-ArchivesPublications@nrc-cnrc.gc.ca.

# RESPONSE SURFACE MODELS FOR THE HYDRODYNAMIC LOADS MEASURED ON SLENDER UNDERWATER VEHICLES DURING PURE YAW MANOEUVRES

F. Azarsina<sup>1</sup>, C.D. Williams<sup>2</sup> and R. Bachmayer<sup>2</sup>

<sup>1</sup> PhD Candidate, Faculty of Engineering and Applied Science,  
Memorial University of Newfoundland (MUN)  
St. John's, Newfoundland, Canada, A1B 3X5  
e-mail: Farhood.Azarsina@nrc.ca

<sup>2</sup> Research Engineer, National Research Council Canada (NRC),  
Institute for Ocean Technology (IOT)  
St. John's, Newfoundland, Canada, P.O. Box 12093, Station A  
St. John's, Newfoundland, Canada, A1B 3T5  
e-mail: Christopher.Williams@nrc-cnrc.gc.ca  
e-mail: Ralf.Bachmayer@nrc-cnrc.gc.ca

## ABSTRACT

Experiments were performed at the NRC-IOT with the bare hull of a full-scale, slender, body-of-revolution underwater vehicle of five different lengths, using an internal three-component balance and a planar motion mechanism (PMM). The experiments included resistance, static yaw, dynamic sway and yaw, and, circular arc runs. The data from the pure yaw (zigzag) captive manoeuvring tests were used to develop regression equations in the form of Response Surface Models (RSMs) for the hydrodynamic loads versus manoeuvre inputs. A sample application of the RSMs is illustrated in comparison with sea-trials data from the underwater vehicle "MUN Explorer".

## 1. INTRODUCTION

The response surface method is a later outcome of the statistical design of experiment methodology which was innovated and used first in the agricultural sciences in the 1920s [1]. The response surface method or model (RSM) dates from the 1950s. Its early applications were in the chemical industry, but currently it is widely used in quality improvement, product design, uncertainty analysis, etc [2]. In statistical terms, an RSM is a two-factor factorial design augmented with axial runs so as to capture the curvature of the response. However, in a more general form an RSM is a regression model based on factor effects including the interaction effects of the factors.

In order to study the time-varying hydrodynamic loads which are experienced by a fully-submerged underwater vehicle, one way is to perform captive-model forced oscillations with a device such as a Planar Motion Mechanism (PMM). In practice it is

convenient (for programming of the drive motions, smoothness of the loads imposed on the PMM, and, for data-analysis purposes) to use sinusoidal motions. In a spatial coordinate system, such as a towing tank, a sinusoidal trajectory can be defined by the width of one cycle of the trajectory (cycle-width) and the amount of length of towing tank required to execute one cycle, the cycle-length. In the context of the motions of the PMM and the towing carriage, the cycle width is equivalent to the amplitude of the lateral (sway) motion  $A$ , and the cycle-length is equivalent to the product  $T \cdot u_{\text{carriage}}$  where  $T$  is the period of the motion and  $u_{\text{carriage}}$  is the constant carriage speed.

As a part of the underwater vehicle hydrodynamics research at NRC-IOT and MUN, the pure sway and pure yaw (zigzag) experiments on a series of five hull forms for an axi-symmetric underwater vehicle were performed in the 90 m towing tank at NRC-IOT. These experiments used the towing carriage to move the vehicle along the tank x-axis, the PMM to produce the oscillating lateral (sway) plus angular (yaw) motions, and, an internal three-component balance to measure two hydrodynamic forces (axial, lateral) and the hydrodynamic yaw moment. See Table I at the end for the details of the pure yaw manoeuvres.

In this paper, the resulting experimental data from the pure yaw (zigzag) captive manoeuvring experiments are used to develop regression equations in the form of RSMs for the hydrodynamic loads versus manoeuvre inputs. The RSMs can then be used to predict the hydrodynamic loads for a range of bare-hull dimensions and manoeuvring missions. A sample application of the RSMs is illustrated in comparison with sea-trials data from the underwater vehicle "MUN Explorer".

## 2. EXPERIMENTAL RESULTS FOR THE PURE YAW MANOEUVRES

The original bare-hull model of the underwater vehicle had a length-to-diameter ratio ( $l/d$ ) of about 8.5:1. Extension pieces were added to the parallel mid-body to test hulls of the same diameter, 203 mm, but with  $l/d$  of 9.5, 10.5, 11.5 and 12.5 [3]. Fig. 1 shows the five hull-series.

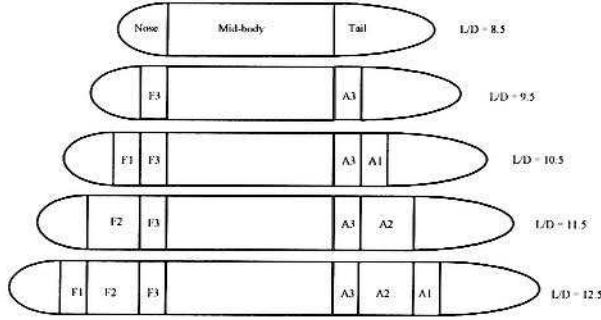


Fig. 1. The five hull-series configuration [3]

The carriage forward velocity for all the pure yaw runs was 2 m/s; the sway velocity and yaw angle of the PMM had smooth sinusoidal variations with amplitudes of about 0.5 m/s and 14 deg for all the runs. The maximum and minimum sway motion amplitudes were 1.25 and 0.41 m. The maximum and minimum yaw rates were respectively about 17 deg/s for the shortest model in its short-period zigzag motion, and, about 5.5 deg/s for the longest model in its long-period zigzag manoeuvre.

During a pure yaw manoeuvre the longitudinal axis of the vehicle is everywhere tangent to the sinusoidal trajectory in the tank ( $x,y$ ) coordinate system. In these zigzag manoeuvres, the yaw angle and sway velocity of the PMM are in phase with each other, and the periods of the yaw and sway motions are identical. In our experiments, all the runs were designed for constant amplitude of yaw angle and sway velocity of the PMM, but of varying amplitude of the sway displacement. Therefore, the smaller displacement pure yaw manoeuvres were of shorter period and had larger yaw rates of turn.

For the pure yaw manoeuvres the input signals to the PMM are the time-series of PMM lateral velocity,  $v(t)$  and model heading angle,  $\beta(t)$ . The main responses to be studied in the pure yaw experiments are the sway force,  $F_Y$ , and yaw moment,  $M_Z$ . Fig. 2 shows a sample yaw angle signal for a  $l/d$  of 8.5 and input values  $A$  of 0.51 m and  $T$  of 6.4 s; Fig. 3 shows the filtered sway force  $F_Y$ .

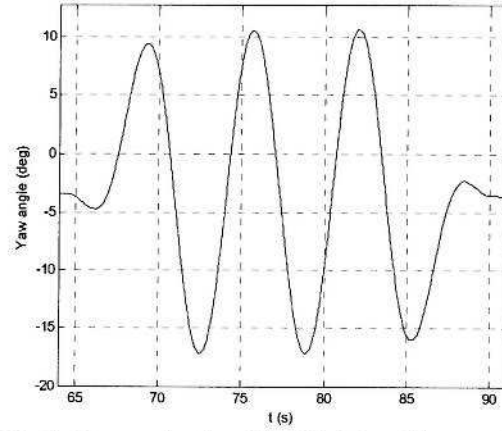


Fig. 2. Yaw angle signal for  $l/d=8.5$  and input values of  $A=0.51$  m and  $T=6.4$  s for a pure yaw manoeuvre

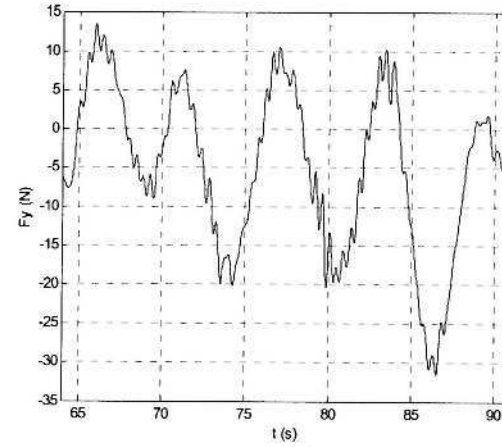


Fig. 3. The filtered sway force signal during the pure yaw manoeuvre of Fig. 2

The amplitude of force and moment sinusoidal signals, named  $F_{Y0}$  and  $M_{Z0}$ , are non-dimensionalized as follows:

$$F_{Y0}' = F_{Y0} / [(1/2)\rho U^2 A_p] \quad (1)$$

and

$$M_{Z0}' = M_{Z0} / [(1/2)\rho U^2 A_p l] \quad (2)$$

where  $\rho$  is the water density,  $A_p$  is the planform area of the vehicle defined as:

$$A_p = l \cdot d, \quad (3)$$

and  $U$  is the vehicle velocity evaluated as:

$$U^2 = u_{\text{carriage}}^2 + v_0^2 \quad (4)$$

where  $u_{\text{carriage}}$  is the towing speed of the carriage which was 2 m/s for all the pure yaw runs, and  $v_0$  is the amplitude of PMM sinusoidally-varying lateral velocity which was 0.5 m/s for all runs.

Plotting the experimental data for the amplitude of the non-dimensional sway force and yaw moment versus non-dimensional sway amplitude  $A/d$  during pure yaw runs, showed a clear trend: the short-period small-amplitude manoeuvres result in larger loads and

the long-period high-amplitude runs result in smaller loads [4].

There is also a phase lag between the input signals of the zigzag motion and the response signals of force and moment. Plotting  $\phi_F$ , the phase lag between  $FY$  and  $\beta$ , in radians, versus  $A/d$  for the pure yaw manoeuvres with this hull-series, revealed that the sinusoidal sway force is delayed by about  $\pi/2$  radians relative to the sinusoidal yaw angle. Although, the data were scattered, there is a trend: the longer vehicle experiences a larger phase lag and for slower manoeuvres (larger  $A/d$ ) the phase lag is larger. For the phase lag between  $MZ$  and  $\beta$ , namely  $\phi_M$ , versus  $A/d$  for the hull-series, again the trend is that the longer hull  $l/d$  experiences a larger phase difference, and for long-period manoeuvres (larger  $A/d$ ) the phase lag is larger.

In summary, from our preliminary analysis the following observations were made [4]:

a. For a fixed hull length, the smaller displacement manoeuvres were of shorter period and had larger yaw rates of turn, and the smaller displacement manoeuvres resulted in larger measured hydrodynamic loads.

b. For the series of five hull lengths, vehicles with larger length-to-diameter ratio experienced larger measured hydrodynamic loads.

c. The phase lag between the time-series of two of the manoeuvre inputs (yaw angle and sway velocity) and the time-series of the measured loads were summarized in terms of vehicle length-to-diameter ratio and these inputs. These results provide information concerning the effects of hull length on the added-mass and added moment of inertia [4].

### 3. THE MATHEMATICAL MODEL

A mathematical model for the experimental results of the pure yaw manoeuvres is desired. According to the previous section, the input signals for these zigzag manoeuvres are the sway velocity and yaw angle of the PMM which can be written as:

$$v = v_0 \sin(\omega_v t) \quad (5)$$

$$\beta = \beta_0 \sin(\omega_\beta t) \quad (6)$$

where the sway velocity amplitude  $v_0$  was 0.5 m/s, and the yaw angle amplitude  $\beta_0$  was 14 deg. The frequencies of the two motions, sway and yaw, must be identical, thus  $\omega = \omega_v = \omega_\beta$ , and in phase with each other. On the other hand, measurements reveal that the frequency of the hydrodynamic loads is the same as frequency of the input signals. Therefore the sway force and yaw moment are of the form:

$$FY = FY_0 \sin(\omega t - \phi_F) \quad (7)$$

$$MZ = MZ_0 \sin(\omega t - \phi_M) \quad (8)$$

The measured response sway force,  $FY$ , in a captive zigzag manoeuvre in towing tank, for a range

of different hull lengths, can be written as:

$$FY = f(u_{\text{carriage}}, v, \beta, \dot{\beta}, A/d, l/d) \quad (9)$$

We are interested in what are the hydrodynamic loads acting on the hull of a fully-submerged underwater vehicle during abrupt manoeuvres. Unlike during turning circles where the yaw rate is constant, in a spatially-sinusoidal manoeuvre the turning rate changes continuously. Thus we are interested in manoeuvres which produce rapid turning rates, and portions of sinusoidal pure yaw manoeuvres fulfil that requirement.

During a sea-trial, an overhead view of a spatially-sinusoidal trajectory allows us to view the cycle width and cycle length; these are analogous to the PMM sway amplitude and cycle length  $T \cdot u_{\text{carriage}}$  in the towing tank. In designing the pure yaw manoeuvres there are several constraints that must be satisfied. Two are due to physical limitations of the PMM (i) the maximum sway velocity cannot exceed 0.50 m/s, and, (ii) the maximum yaw rate cannot exceed 60 deg/sec. The first of these requires that:

$$A \cdot \omega < 0.50 \text{ [m/s]} \quad (10)$$

or, which is equivalent, that

$$T > 4\pi \cdot A \text{ [sec]} \quad (11)$$

A third constraint is the kinematic requirement that the longitudinal axis of the vehicle is everywhere tangent to the sinusoidal trajectory in the tank ( $x, y$ ) coordinate system; this requires that

$$\beta_0 = \arctan[\omega \cdot A / u_{\text{carriage}}] \quad (12)$$

which is equivalent to

$$\beta_0 = \arctan[2\pi \cdot A / (T \cdot u_{\text{carriage}})] \quad (13)$$

In these experiments we used a constant carriage speed of 2 m/s. Combining these kinematic and dynamic constraints, the result is that:

$$\beta_0 < \arctan(1/4) \quad (14)$$

so the yaw amplitude will not exceed about 14 deg in any of these pure sway manoeuvres.

For small yaw amplitudes (13) can be approximated by:

$$\beta_0 \approx 2\pi A / (T \cdot u_{\text{carriage}}) \quad (15)$$

or

$$T \approx 2\pi A / (\beta_0 \cdot u_{\text{carriage}}) = 2\pi d \cdot (A/d) / (\beta_0 \cdot u_{\text{carriage}}) \quad (16)$$

If the carriage speed  $u_{\text{carriage}}$  and yaw amplitude  $\beta_0$  are held constant at 2 m/s and 14 deg respectively, then (16) provides a linear relation between the period  $T$  and the sway amplitude  $A$  or non-dimensional sway amplitude  $A/d$ .

The time-series for the PMM sway and yaw motions for each of the 11 runs with the shortest model were plotted as in Fig. 2, for one or more cycles of motion; smooth sinusoids (5) and (6) were fitted to the constant-amplitude portions of the time-series and values for  $\beta_0$ ,  $T$  and  $A$  were extracted. These experimental values are plotted in Fig. 4. This plot confirms the validity of the approximation (16).



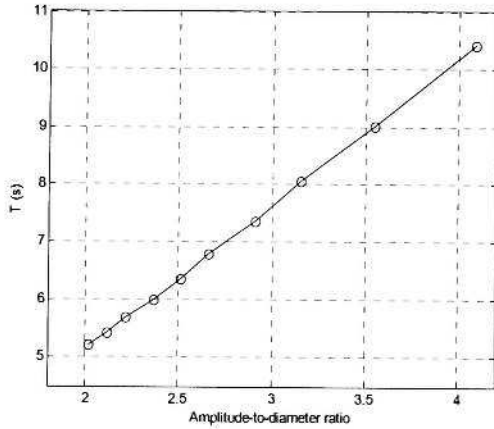


Fig. 4. Time period versus sway amplitude  $A/d$ ; pure yaw runs for  $l/d=8.5$

Therefore, using (5) and (6), equation (9) reduces to:

$$FY = f(\omega, t, A/d, l/d) \quad (17)$$

The relation in Fig. 4 can usefully be represented by a straight line through the origin which expresses the relation:

$$A/T \approx 0.078 \text{ [m/s]} \quad (18)$$

or

$$A \cdot \omega \approx 0.489 \text{ [m.rad/s]} \quad (19)$$

which satisfies the requirement in (10) that the maximum sway velocity cannot exceed 0.50 m/s. Hence, (17) can be further simplified to

$$FY = f(t, A/d, l/d) \quad (20)$$

These results show that in the constant-amplitude portion of each pure yaw run, the complicated relation (9) reduces to the simpler relation (20). The same observation applies to the yaw moment  $MZ$ , thus:

$$MZ = g(t, A/d, l/d) \quad (21)$$

Using (7) and (8), equations (17) and (20) decompose into the following set of equations which are time-independent:

$$FY_0 = f_1(A/d, l/d), \quad \varphi_F = f_2(A/d, l/d) \quad (22)$$

$$MZ_0 = g_1(A/d, l/d), \quad \varphi_M = g_2(A/d, l/d) \quad (23)$$

This gives a mathematical model for the zigzag tests under study; we seek smooth expressions for  $f_1, f_2, g_1$  and  $g_2$ . It should be noted that the mathematical model is constrained by equation (18).

#### 4. RESPONSE SURFACE MODELS

A regression model for a response, which depends on two factors, is a surface in 3D space. The response surface may be represented graphically using a contour plot or a 3-D plot; this type of graphical representation is possible only when there are two factors. In the contour plot, lines of constant response are drawn in the plane of the two factors. In a 3D representation, the response is plotted in the third

dimension. The Response Surface Model (RSM) can be a first-order model if the response is a linear function of the factors. If the response has curvature, then a higher order polynomial should be used. A second-order (quadratic) model is often able to capture the curvature. The general form of a quadratic regression for the response  $z$  versus the factors  $x$  and  $y$  is written as:

$$z = C_{xx}x^2 + C_{yy}y^2 + C_{xy}x \cdot y + C_x x + C_y y + C \quad (24)$$

where  $C_{xy}$  represents the interaction effect between the two factors in the response. We are looking for the regression coefficients in (24) to make a model for (22) and (23).

##### A. Regression model for the sway force amplitude

First, the sway force in equation (22) is studied. For the non-dimensional sway force amplitude Fig. 5 shows quadratic curves fitted to the test data. The fitted curves are of the following quadratic regression form:

$$1000 \cdot FY_0' = p_1 \cdot (A/d)^2 + p_2 \cdot (A/d) + p_3 \quad (25)$$

Table II shows the regression coefficients for the five hull models. The quadratic curves in Fig. 5 are approximately parallel to each other, which mean that there is only a small interaction effect in the response sway force amplitude between the two factors sway amplitude and vehicle length. That is, whether the vehicle length is large or small, the relationship between sway force amplitude and sway amplitude is almost the same only shifted vertically.

Since the curves have approximately the same trend, an average quadratic curve is plotted with bold solid line in Fig. 5, the coefficients of which are the average of the coefficients in Table II for the four longest models. The average curve is:

$$1000 \cdot FY_0' = 0.7 \cdot (A/d)^2 - 9.75 \cdot (A/d) + 44.94 \quad (26)$$

Now if (25), with coefficients in Table II, is used to make a new plot of the non-dimensional sway force amplitude in which length-to-diameter ratio is on the x-axis, a plot as in Fig. 6 is obtained. Different markers represent different non-dimensional sway amplitude values from two to six. As can be observed the variation of the non-dimensional sway force amplitude versus length-to-diameter ratio is almost linear for all sway amplitudes.

Table II. Regression coefficients for the five hull series for the quadratic fit in equation (25)

$l/d$	$p_1$	$p_2$	$p_3$	R-square
8.5	2.29	-18.5	52.07	0.933
9.5	0.61	-8.43	40.21	0.981
10.5	0.89	-11	46.77	0.991
11.5	0.76	-10.84	48.33	0.987
12.5	0.54	-8.71	44.46	0.95

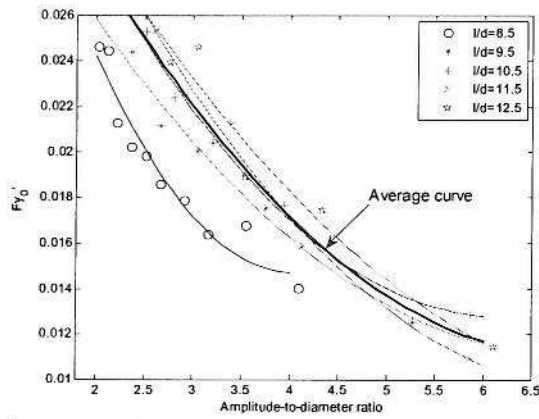


Fig. 5. Non-dimensional sway force amplitude vs.  $A/d$  during pure yaw manoeuvres

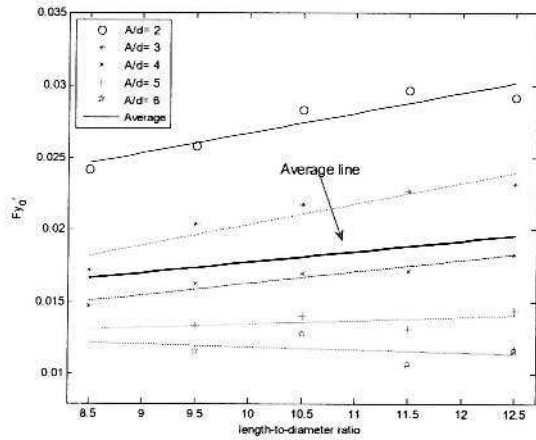


Fig. 6. Non-dimensional sway force amplitude vs.  $l/d$  during pure yaw manoeuvres

The average linear variation of sway force amplitude versus length-to-diameter ratio is shown by the bold solid line in Fig. 6, which has the following regression equation:

$$1000 \cdot FY_0' = 0.73 \cdot (l/d) + 10.45 \quad (27)$$

On the other hand, the lines in Fig. 6 are approximately parallel to each other, which again proves that there is only a small interaction effect on the response sway force amplitude between the factors sway amplitude and vehicle length. That is, whether the sway amplitude is large or small, the effect of vehicle length on the sway force amplitude is almost the same.

Going back to the regression coefficients in (24), for the sway force amplitude, combining (26) and (27), the following model is derived:

$$1000 \cdot FY_0' = 0.7 \cdot (A/d)^2 - 9.75 \cdot (A/d) + 0.73 \cdot (l/d) + C \quad (28)$$

where  $2 < (A/d) < 6$  and  $8.5 < (l/d) < 12.5$ . Calibrating (28) with the experimental data results in a value of 36.80 for the intercept  $C$ . Note that the intercept value

does not mean that the sway force for zero sway amplitude is non-zero; the RSM is not valid for extrapolation outside the range of variation of  $A/d$  as stated above.

It is convenient to convert the actual values of the two factors to coded levels. The coded factors are defined so as the low and high levels are minus one and plus one, respectively. It is easier to work with the data if they are scaled to have zero mean and unit standard deviation. Hence, if the coded factors  $A/d$  and  $l/d$  are named respectively  $X$  and  $Y$  varying from  $-1$  to  $1$ , as shown in Table III, then (28) changes to:

$$1000 \cdot FY_0' = 2.8 \cdot X^2 - 8.3 \cdot X + 1.46 \cdot Y + C \quad (29)$$

Note that the intercept  $C$ , in (28) and in (29) have different values; the intercept in (29) has the value 16.66.

The advantage of working with the coded factors is that one can directly compare the regression coefficients to see which factor has a more significant effect on the response. According to (29), factor  $X$ , the sway amplitude, has a linear effect of about six times larger than the factor  $Y$ , the vehicle length, on the response sway force amplitude. Moreover, factor  $X$  is the source of curvature in the response surface. The response surface for the sway force amplitude when plotted versus the coded factors is shown in Fig. 7. Note that the centre-point in Fig. 7,  $[X, Y] = [0, 0]$  corresponds to the actual values  $[A/d, l/d] = [4, 10.5]$ . The largest force amplitude is at the corner:  $[X, Y] = [-1, 1]$  which corresponds to:  $[A/d, l/d] = [2, 12.5]$ , that is, the longest hull in the most rapid zigzag manoeuvre experiences the largest force.

Table III. Actual and coded factors

$A/d$	2	3	4	5	6
$X$	-1	-0.5	0	0.5	1
$l/d$	8.5	9.5	10.5	11.5	12.5
$Y$	-1	-0.5	0	0.5	1

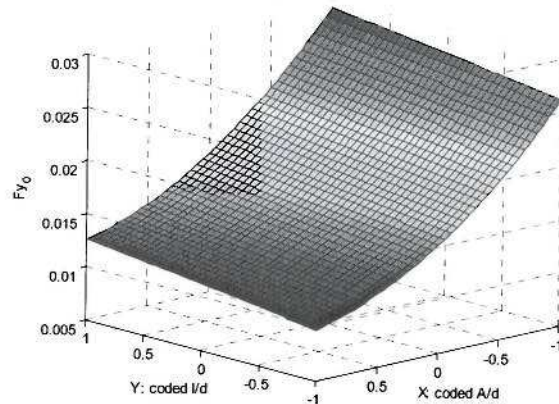


Fig. 7. Response surface for the non-dimensional sway force amplitude in zigzag manoeuvres



### B. Regression model for the yaw moment amplitude

Next the yaw moment amplitude in equation (23) is modeled through the same process as for the sway force. Therefore, first a quadratic regression is performed over the factor sway amplitude, which is followed by a linear regression over the factor length-to-diameter ratio. The results are shown in Figs. 8 and 9. Again the average variation is shown with a bold solid line. The equations for the average quadratic curve in Fig. 8 and the average line in Fig. 9 are respectively:

$$1000 \cdot MZ_0' = 0.34 \cdot (A/d)^2 - 3.86 \cdot (A/d) + 12.16 \quad (30)$$

and

$$1000 \cdot MZ_0' = 0.22 \cdot (l/d) + 0.43 \quad (31)$$

Using (24), (30) and (31) results in the following regression model for the yaw moment amplitude:

$$1000 \cdot MZ_0' = 0.34 \cdot (A/d)^2 - 3.86 \cdot (A/d) + 0.22 \cdot (l/d) + C \quad (32)$$

The test data provide a value of 9.9 in (32) for the intercept C.

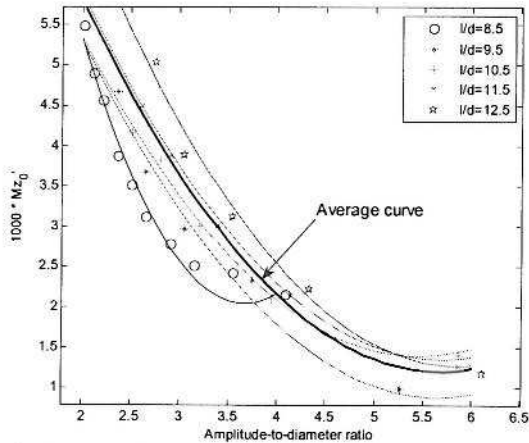


Fig. 8. Non-dimensional yaw moment amplitude vs.  $A/d$  during pure yaw manoeuvres

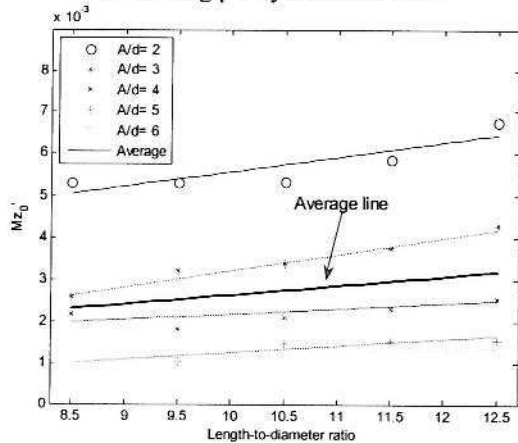


Fig. 9. Non-dimensional sway force amplitude vs.  $l/d$  during pure yaw manoeuvres

As in the previous section for the sway force amplitude, also for the regression model of the yaw moment amplitude, equation (32), there is no term for the interaction effect of the two factors, sway amplitude and vehicle length, which is reasonable due to the parallel curves in both Figs. 8 and 9. Physically it means that no matter what is the vehicle length, the sway motion amplitude has approximately the same effect on the yaw moment amplitude, and vice versa.

The regression model in (26) can be rewritten for the coded factors X and Y, as defined before, hence:

$$1000 \cdot MZ_0' = 1.36 \cdot X^2 - 2.28 \cdot X + 0.44 \cdot Y + C \quad (33)$$

The value for the intercept in the coded equation (33) is 2.21. As mentioned previously, the response model for the coded factors reveals the relative significance of the effect of each term. The linear effect of the sway motion amplitude on the yaw moment amplitude is about five times of the effect of hull length; also the sway amplitude is the source of curvature in the response surface. The RSM is shown in Fig. 10.

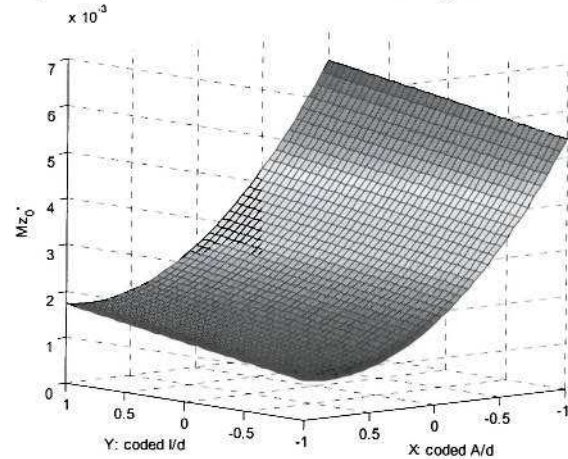


Fig. 10. Response surface for the non-dimensional yaw moment amplitude in zigzag manoeuvres

### B. The phase lag between manoeuvre inputs and hydrodynamic loads

It is more difficult to model the phase lags. As was introduced in section 2, the sinusoidal sway force is delayed by a phase angle  $\varphi_F$  of about  $\pi/2$  radians relative to the sinusoidal yaw angle, and for the yaw moment the phase lag,  $\varphi_M$ , is close to zero, though it gets as large as 0.7 radians for the long hulls in slow zigzags. Figs. 11 and 12 show the experimental data for the hull-series for the sway force and yaw moment phase lags. Because of the scattered data the procedure that was used before in sections 4A and 4B to fit a response surface model does not work in this case. The curves fitted to the data only show the general trend for all hull series [4]. The fitted curves in Figs. 11 and 12 are the following quadratic

equations respectively:

$$\varphi_F = -0.045 \cdot (A/d)^2 + 0.41 \cdot (A/d) + 0.72 \quad (34)$$

$$\varphi_M = -0.0084 \cdot (A/d)^2 + 0.194 \cdot (A/d) - 0.257 \quad (35)$$

The above assumption is not very realistic, because as can be seen from the experimental data the phase lag depends on the vehicle length-to-diameter ratio as well.

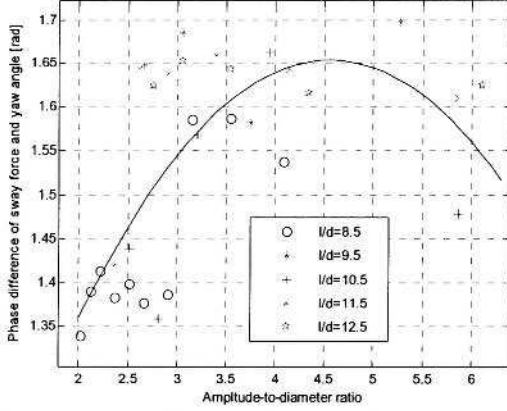


Fig. 11. Phase difference of FY and  $\beta$  vs. A/d during pure yaw manoeuvres

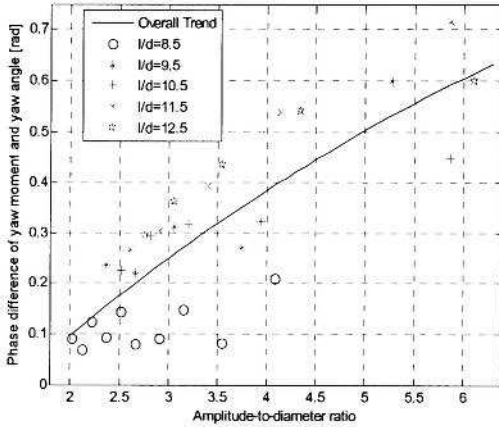


Fig. 12. Phase difference of MZ and  $\beta$  vs. A/d during pure yaw manoeuvres

## 5. THE APPLICATION OF THE RESPONSE SURFACE MODELS

### A. The constraint

It should be recalled that the mathematical model used in this study and the response surface models based on that, are subject to a very important constraint, that is, equation (18) restated as follows:

$$A/T = 0.078 \text{ [m/s]}. \quad (18)$$

This constraint says that the zigzag tests of this study, which were first reported in [4], are of relatively short period and abrupt.

For comparison we investigate a zigzag manoeuvre run that was performed by the MUN *Explorer* underwater vehicle, in order to clarify the

applicability of the RSMs that are being developed in this paper. The MUN *Explorer* is a survey-class autonomous underwater vehicle (AUV) owned by Memorial University of Newfoundland. It is 4.5 m in length with a maximum diameter of 0.69 m and is designed to go as deep as 3000 m with cruising speeds between 0.5 and 2.5 m/s.

In a series of free-running manoeuvring experiments that were performed by the MUN *Explorer* AUV in summer 2006 in the open ocean, there were some zigzag manoeuvres, both in horizontal and vertical planes. Reported in [5] is a horizontal zigzag manoeuvre, that is, a zigzag manoeuvre at a constant depth of about three metres with commanded amplitude and cycle-length of 20 m and 80 m respectively, at a forward speed of 1.5 m/s. An overshoot of about eight metres in amplitude was observed, therefore the parameters for this zigzag are:

$$A = 28 \text{ [m]}, U = 1.5 \text{ [m/s]}, T = 80/1.5 = 53.3 \text{ [s]}, \\ l/d = 6.5, A/d = 40.6 \quad (36)$$

which results in:

$$A/T = 0.525 \text{ [m/s]}. \quad (37)$$

In comparison with (18), the constraint of the mathematical model in this research, for the same sway amplitude, (37) indicates that the zigzag manoeuvre performed by the MUN *Explorer* AUV is about seven times slower than the one in this paper. Note that the l/d ratio at 6.5 for the MUN *Explorer* is outside the range of applicability  $8.5 < l/d < 12.5$  of our response model. Similarly the value of A/d of 40.6 is outside the range of applicability of  $2 < A/d < 6.1$  used in this study. It is postulated that the linear effects of length-to-diameter ratio exhibited in expressions (28) and (29) will permit an extrapolation to 6.5 based on the validated range of 8.5 to 12.5. However the quadratic effect of sway amplitude prevents extrapolation to A/d of 40.6 which is well beyond the validated range of 2 to 6.1.

Due to these considerations, these RSMs are not suitable for estimating the sway force and yaw moment exerted on the MUN *Explorer* in the above zigzag manoeuvre.

### B. Sample application

For a sample application of the RSMs, imagine a zigzag manoeuvring mission to be performed by the MUN *Explorer* AUV defined as follows: commanded amplitude and cycle-length for the zigzag equal to 4 m and 50 m respectively with a forward speed of 1.5 m/s. Such an abrupt manoeuvre may occur, for example, during obstacle avoidance such as manoeuvring around a small iceberg. For this abrupt turn:

$$A = 4 \text{ [m]}, U = 1.5 \text{ [m/s]}, T = 50/1.5 = 33.3 \text{ [s]} \quad (38)$$



In this case we have:  $A/T = 0.12$  [m/s], which is close to 0.078 in the mathematical model of this study. Converting the variables sway amplitude and vehicle length to their coded form result in:

$$l/d = 6.5 \rightarrow Y = -2, A/d = 5.8 \rightarrow X = 0.9 \quad (39)$$

The coded factor  $Y$  is out of the original range  $[-1,1]$ , but because its effect is linear it should predict the response correctly. Inserting  $X$  and  $Y$  into (29) and (33) gives:

$$FY_0' = 8.5 \cdot 10^{-3} \text{ and } MZ_0' = 0.4 \cdot 10^{-3} \quad (40)$$

For the MUN *Explorer* the non-dimensionalizing factor in equations (1) and (2), is found to be:

$$(1/2)\rho U^2 A_p = (1/2) \cdot 1025 \cdot (1.5^2) \cdot 4.5 \cdot 0.69 = 3580 \quad (41)$$

For the yaw moment, (41) should be multiplied by the length of the vehicle again. Therefore, the sway force and yaw moment amplitudes exerted on this AUV in such a manoeuvre are:

$$FY_0 = 30.43 \text{ [N]} \text{ and } MZ_0 = 6.44 \text{ [N.m]} \quad (42)$$

The force and moment in (40) are estimates of the total hydrodynamic sway force and yaw moment that are exerted on the bare hull of this AUV in such a zigzag mission, considering that the bare hull of the MUN *Explorer* and the hull-series of this study are both streamlined and axi-symmetric with similar shapes but different dimensions.

The yaw angle amplitude for this zigzag manoeuvre is derived using the approximation (15) as follows:

$$\beta_0 = 2\pi A / (T \cdot u_{\text{carriage}}) = 0.503 \text{ [rad]} = 28.8 \text{ [deg]} \quad (43)$$

Hence, the maximum lateral speed, namely the amplitude of the sway velocity in the global coordinate system is:

$$v_0 = U \cdot \sin(\beta_0) = 0.72 \text{ [m/s]} \quad (44)$$

The phase lag between the yaw angle signal and hydrodynamic loads are estimated using (28) and (29) as follows:

$$\varphi_F = 90.77 \text{ [deg]}, \varphi_M = 33.55 \text{ [deg]} \quad (45)$$

The MUN *Explorer* AUV has two rudders with symmetric NACA 0024 profile, with chord, span and thickness of respectively

$$c = 0.35 \text{ m}, b = 0.25 \text{ m}, t = 0.24 \cdot c = 0.084 \text{ m} \quad (46)$$

The moment arm of the rudders (distance between centre of pressure of the rudders and centre of gravity of the vehicle) is about  $d_{\text{rudders}} = 1.2$  m. The total turning moment provided by the two rudders is estimated to be given by

$$MZ_{\text{rudders}} = 2 \cdot (1/2)\rho U^2 \cdot b \cdot c \cdot C_L \cdot d_{\text{rudders}} \quad (47)$$

Here the lift coefficient for NACA 0024 with an angle of attack relative to the local flow direction of  $\delta$  [deg] is approximately equal to [6]:

$$C_L = 0.080 \cdot \delta \quad (48)$$

Summarizing (46) to (48) we estimate that

$$MZ_{\text{rudder}} = 19.37 \cdot \delta \text{ [N.m]} \quad (49)$$

Using (42) and (49), assuming that (42) is the total moment opposing the turn, results in:

$$I\ddot{\beta} = 19.37 \cdot \delta - 6.44 \quad (50)$$

The moment of inertia of the vehicle, denoted by  $I$ , still has not been measured but using the tabular data in the software developed in [7], for a submarine of the same size with a uniform mass distribution, the moment of inertia  $I$  is estimated to be  $1200 \text{ [kg.m}^2\text{]}$ . With the payload installed, the dry weight of the vehicle is 606 kg.

The yaw angular acceleration in (50) is calculated using (6) as follows:

$$\ddot{\beta} = -\beta_0 \cdot \omega^2 \sin(\omega t) \quad (51)$$

Figs. 13 and 14 respectively show the yaw angle signal and the yaw moment signal for this zigzag manoeuvre with the MUN *Explorer* AUV with a commanded amplitude and cycle-length for the zigzag equal to 4 m and 50 m respectively. In Fig. 14 the yaw angle signal is shown again by the dashed line; its amplitude is scaled to the amplitude of the yaw moment signal.

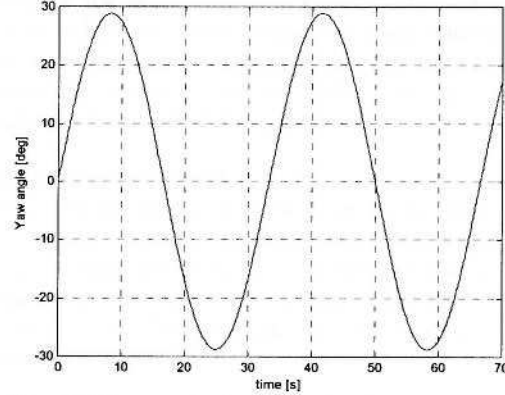


Fig. 13. Yaw angle signal for the zigzag manoeuvre with the MUN *Explorer* AUV

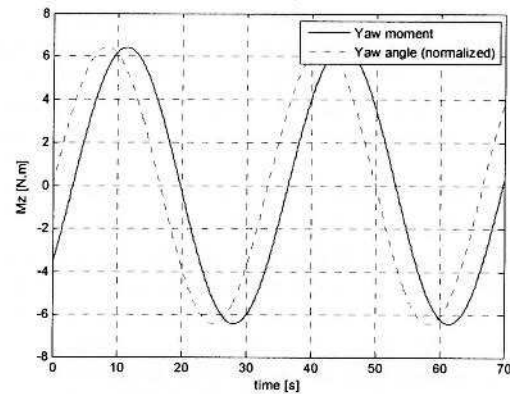


Fig. 14. Yaw moment signal for the zigzag manoeuvre with the MUN *Explorer* AUV

According to Fig. 14, when the yaw moment signal is maximum, at time  $t_{MZ}$ , the yaw angle signal (and the yaw angular acceleration  $\ddot{\beta}$ ) is below its

Table I. Settings for all the runs of pure yaw manoeuvres

Model length-to-diameter ratio	Run Number	PMM sway amplitude [m]	Non-dimensional PMM sway amplitude $A/d$	PMM sway & yaw period [sec]	Approximate yaw amplitude [rad]	Approximate yaw amplitude [deg]	Max PMM sway velocity [m/s]	Approx max PMM yaw rate [deg/sec]
8.5	177	0.413	2.04	5.20	0.25	14.3	0.50	17.3
8.5	176	0.432	2.13	5.43	0.25	14.3	0.50	16.6
8.5	175	0.453	2.23	5.69	0.25	14.3	0.50	15.8
8.5	174	0.477	2.35	6.00	0.25	14.3	0.50	15.0
8.5	173	0.506	2.49	6.36	0.25	14.3	0.50	14.1
8.5	172	0.541	2.67	6.80	0.25	14.3	0.50	13.2
8.5	171	0.585	2.88	7.35	0.25	14.3	0.50	12.2
8.5	170	0.641	3.16	8.05	0.25	14.3	0.50	11.2
8.5	169	0.716	3.53	9.00	0.25	14.3	0.50	10.0
8.5	168	0.827	4.07	10.4	0.25	14.3	0.50	8.7
8.5	167	1.013	4.99	12.7	0.25	14.3	0.50	7.1
9.5	164	0.480	2.36	6.04	0.25	14.3	0.50	14.9
9.5	163	0.537	2.65	6.75	0.25	14.3	0.50	13.3
9.5	162	0.620	3.05	7.79	0.25	14.3	0.50	11.6
9.5	165	0.620	3.05	7.79	0.25	14.3	0.50	11.6
9.5	161	0.760	3.74	9.53	0.25	14.4	0.50	9.5
9.5	160	1.074	5.29	13.5	0.25	14.3	0.50	6.7
10.5	146	0.506	2.49	6.36	0.25	14.3	0.50	14.1
10.5	144	0.654	3.22	8.21	0.25	14.3	0.50	11.0
10.5	145	0.654	3.22	8.21	0.25	14.3	0.50	11.0
10.5	142	0.801	3.95	10.1	0.25	14.3	0.50	9.0
10.5	143	0.801	3.95	10.1	0.25	14.3	0.50	9.0
10.5	140	1.132	5.58	14.2	0.25	14.3	0.50	6.3
10.5	141	1.132	5.58	14.2	0.25	14.3	0.50	6.3
11.5	158	0.531	2.62	6.66	0.25	14.4	0.50	13.5
11.5	157	0.594	2.93	7.45	0.25	14.4	0.50	12.1
11.5	156	0.686	3.38	8.61	0.25	14.3	0.50	10.5
11.5	155	0.840	4.14	10.6	0.25	14.3	0.50	8.5
11.5	154	1.188	5.85	14.9	0.25	14.3	0.50	6.0
12.5	152	0.555	2.73	6.96	0.25	14.4	0.50	13.0
12.5	151	0.620	3.05	7.79	0.25	14.3	0.50	11.6
12.5	150	0.716	3.53	9.00	0.25	14.3	0.50	10.0
12.5	149	0.877	4.32	11.0	0.25	14.3	0.50	8.2
12.5	148	1.240	6.11	15.6	0.25	14.3	0.50	5.8



maximum value, therefore the angular acceleration that should be substituted into (50) is:

$$\ddot{\beta}(t_{MZ}) = -\beta_0 \cdot \omega^2 \sin(\varphi_M) =$$

$$0.503 \cdot (2\pi/33.33)^2 \cdot 0.55 = 9.83 \cdot 10^{-3} [\text{rad/s}^2] \quad (52)$$

Substituting (52) and the estimated moment of inertia into (50) results in:

$$I\ddot{\beta} = 1200 \cdot 9.83 \cdot 10^{-3} = 19.37 \cdot \delta - 6.44 \quad (53)$$

This allows us to solve for the required amplitude of the deflection angle  $\delta_0$  for this zigzag manoeuvre, which is 0.94 deg. Probably the yaw moment given by the rudders has been overestimated and the total opposing yaw moment underestimated, because there is some efficiency lower than 100% for the rudders, and there is some extra opposing moment in addition to the bare-hull moment evaluated by the RSMs here. In addition (48) assumes that the rudders are operating in a steady-flow regime as would be experienced in a circular-arc turn at constant forward speed, but not during a zigzag manoeuvre where the instantaneous angle of attack and rudder deflection are changing continuously. Also the angle of attack  $\delta$  in (48) should properly account for the true local angle of attack while turning.

## 6. CONCLUSIONS

As a continuation to the preliminary observations and data analysis for the pure yaw manoeuvres for a series of underwater vehicle bare hulls, that were reported previously in [4], Response Surface Models (RSMs) for captive-model zigzag manoeuvres were introduced and developed in this study. The following observations can be made.

a. These set of zigzag manoeuvres were of short period and abrupt, with a constant ratio of manoeuvre amplitude to its period A/T of 0.078. In comparison, a regular free-running zigzag test by the MUN *Explorer* AUV had an A/T value of 0.525. Therefore the results of this paper are mainly valid for rapid turns, e.g. in the case of obstacle-avoidance.

b. The effect of hull length-to-diameter ratio on the hydrodynamic loads exerted on the bare-hull of an underwater vehicle in a short-period zigzag manoeuvre is observed to be a weak linear effect. In contrast, the effect of sway amplitude is much larger in that it has both a linear and a quadratic effect. In the context of an RSM, it is the effect of the sway amplitude that is responsible for the curvature in the RSMs.

c. Based on the experimentally-determined yaw moment RSM which was developed in this study, a method has been outlined for estimating the command

signal required for the control surfaces in order to execute a zigzag manoeuvre by a self-propelled fully-submerged underwater vehicle.

Finally it should be noted that with a comparable amount of time and budget as was used for this set of experiments, using a factorial design for the experiments a wider range of hydrodynamic characteristics of the underwater vehicles in zigzag manoeuvres could be studied. The main point is to remove the restriction of constant A/T used in this study, which requires that the yaw angle amplitude to be an independent variable, while still subject to the dynamic constraints of the PMM. This can be the subject of future PMM experiments.

## ACKNOWLEDGMENT

The authors wish to acknowledge all the NRC- IOT staff and students for their assistance with these experiments, and to express our sincere thanks to the researchers working on the MUN *Explorer* AUV, especially Mr. Manoj Issac who was responsible for the at-sea manoeuvres.

## 7. REFERENCES

- [1] Montgomery, D.C., "Design and Analysis of Experiments", 5th edition, John Wiley & Sons, 2001
- [2] Myers, R. H., Montgomery, D. C., "Response Surface Methodology; Process and product optimization using designed experiments", John Wiley, 1995
- [3] Williams, C.D., Curtis, T.L, Doucet, J.M., Issac, M.T., Azarsina, F., "Effects of Hull Length on the Manoeuvring Characteristics of a Slender Underwater Vehicle", proceedings OCEANS'06 MTS/IEEE-Boston Conference, September 18 to 21, 2006
- [4] Azarsina, F., Williams, C.D., Issac, M.T., "Pure Yaw Experiments on a Series of Hull Forms for an Underwater Vehicle: Hydrodynamic Observations and Analysis", International Symposium on Underwater Technology, Tokyo, Japan, April 17-20, 2007
- [5] Issac, M.T., Adams, S., Moqin, H., Bose, N., Williams, C.D., Bachmayer, R., "Manoeuvring Experiments Using the MUN *Explorer* AUV", International Symposium on Underwater Technology, Tokyo, Japan, April 17-20, 2007
- [6] <http://www.aerospaceweb.org>, visited on July 2007
- [7] Azarsina, F., Bose, N., Sief, M.S., "An Underwater Vehicle Manoeuvring Simulation; Focus on Turning Manoeuvres", The Journal of Ocean Technology, Volume II, Number I, Winter 2007